

Applying Mathematical Tools to Accelerate Vaccine Development: Modeling *Shigella* Immune Dynamics

Courtney L. Davis^{1*}, Rezwanul Wahid², Franklin R. Toapanta², Jakub K. Simon³, Marcelo B. Szein^{2,9}, Doron Levy^{4,9}

1 Natural Science Division, Pepperdine University, Malibu, California, United States of America, **2** Center for Vaccine Development, University of Maryland School of Medicine, Baltimore, Maryland, United States of America, **3** NanoBio Corporation, Ann Arbor, Michigan, United States of America, **4** Department of Mathematics and Center for Scientific Computation and Mathematical Modeling, University of Maryland, College Park, Maryland, United States of America

Abstract

We establish a mathematical framework for studying immune interactions with *Shigella*, a bacteria that kills over one million people worldwide every year. The long-term goal of this novel approach is to inform *Shigella* vaccine design by elucidating which immune components and bacterial targets are crucial for establishing *Shigella* immunity. Our delay differential equation model focuses on antibody and B cell responses directed against antigens like lipopolysaccharide in *Shigella*'s outer membrane. We find that antibody-based vaccines targeting only surface antigens cannot elicit sufficient immunity for protection. Additional boosting prior to infection would require a four-orders-of-magnitude increase in antibodies to sufficiently prevent epithelial invasion. However, boosting anti-LPS B memory can confer protection, which suggests these cells may correlate with immunity. We see that IgA antibodies are slightly more effective per molecule than IgG, but more total IgA is required due to spatial functionality. An extension of the model reveals that targeting both LPS and epithelial entry proteins is a promising avenue to advance vaccine development. This paper underscores the importance of multifaceted immune targeting in creating an effective *Shigella* vaccine. It introduces mathematical models to the *Shigella* vaccine development effort and lays a foundation for joint theoretical/experimental/clinical approaches to *Shigella* vaccine design.

Citation: Davis CL, Wahid R, Toapanta FR, Simon JK, Szein MB, et al. (2013) Applying Mathematical Tools to Accelerate Vaccine Development: Modeling *Shigella* Immune Dynamics. PLoS ONE 8(4): e59465. doi:10.1371/journal.pone.0059465

Editor: Stephen J. Turner, University of Melbourne, Australia

Received: November 26, 2012; **Accepted:** February 11, 2013; **Published:** April 2, 2013

Copyright: © 2013 Davis et al. This is an open-access article distributed under the terms of the Creative Commons Attribution License, which permits unrestricted use, distribution, and reproduction in any medium, provided the original author and source are credited.

Funding: This work was supported in part by a University of Maryland, College Park and University of Maryland, Baltimore (UMCP-UMB) Seed Grant (to DL, JKS, and RW), by Grant Numbers R01CA130817 (to DL), K23AI065759 (to JKS), U19 AI082655 (Cooperative Center for Translational Research in Human Immunology and Biodefense; CCHI, to MBS) and DMS-0758374 (a joint NSF/NIGMS program, to DL). The content is solely the responsibility of the authors and does not necessarily represent the official views of the granting institutions. The funders had no role in study design, data collection and analysis, decision to publish, or preparation of the manuscript.

Competing Interests: JKS is an employee of NanoBio Corporation and works on clinical vaccine development, but is not working on *Shigella* vaccines or mathematical modeling and does not have any financial or non-financial competing interests as defined in PLOS ONE editorial policies. Additionally, this does not alter the authors' adherence to all the PLOS ONE policies on sharing data and materials.

* E-mail: courtney.davis2@pepperdine.edu

⁹ These authors contributed equally to this work.

Introduction

Vaccines protect millions of people from viral and bacterial infections every year [1]. Unfortunately, some diseases have defied all attempts at developing effective vaccines. Major hurdles often include highly diverse pathogen strains, imperfect experimental animal models, and a lack of specific knowledge about how the immune system fights off a given disease [2–4]. Mathematical modeling can help vaccine development by capturing complex immunological dynamics and highlighting which immune components are likely of greater importance in protection and disease clearance from particular pathogens. One disease for which vaccination efforts might greatly benefit from mathematical input is shigellosis, caused by *Shigella*, a bacterium that causes roughly 120 million dysentery infections and kills over 1.1 million people (predominantly young children) worldwide every year [5]. Treatment of shigellosis, which relies on the administration of antibiotics, has become increasingly difficult as resistance to both first- and second-line antibiotics has spread [4]. Thus, prevention

of shigellosis is a public health priority. Unfortunately, no vaccine has been licensed against *Shigella* despite decades of clinical trials [3], and much remains unknown about how the immune system reacts to *Shigella* infections. One major hurdle in vaccine development is that identifying immunological correlates of protection in *Shigella* infections, whether mechanistic or nonmechanistic [6] has proven elusive [3].

In this paper, we create mathematical models of the immune response against *Shigella*, which we use to determine which immune effector mechanisms best confer immunity against *Shigella*. We concentrate our efforts on the humoral immune response, as current vaccines strive to incite protective immunity by eliciting specific memory B cells (B_M) and antibody responses [3,7–10].

Shigella infections occur via fecal-oral transmission [5]. Once ingested, *Shigella* infiltrates the gut epithelium via host M cells, which transport bacteria from the gut lumen to macrophages and other innate immune cells that reside just below the mucosal epithelial barrier in the lamina propria [4,11]. These cells typically engulf bacteria and destroy them inside phagocytic vacuoles;

however, *Shigella* is capable of escaping from these cells to invade epithelial cells from the basolateral side while also inducing macrophages to apoptose [4]. *Shigella* that evades destruction by innate immune cells in the lamina propria can enter epithelial cells, after which it can move freely inside and between epithelial cells as an intracellular pathogen [4,11,12]. It is believed that an innate immune response is rarely sufficient to clear a *Shigella* infection, especially after it enters epithelial cells [9]. However, as the infection progresses, *Shigella* can elicit the induction of antibody responses and effector T cells, as well as memory B and T cells, which typically results in the elimination of the organism [7–10,12,13].

Activated *Shigella*-specific B cells undergo clonal expansion, somatic hypermutation, class switching, and differentiation into antibody-secreting plasma cells (ASC) and B_M cells. Plasma cells initially produce M-type immunoglobulin (IgM); however following class switching, these cells secrete either IgG, the most abundant antibody in serum, or IgA, which is generally accepted to be the most abundant and active antibody isotype at mucosal surfaces [13–16]. IgA, IgG, and IgM antibodies cross the epithelial barrier to function in the lumen. This is accomplished by several mechanisms, including active mechanisms (e.g., poly-Ig receptor (pIgR) transfer for IgM and IgA and the Fc neonatal receptor (FcRn) for IgG) and passive mechanisms (paracellular pathway) for monomeric IgG and IgA [14,15,17]. Once in the lumen, antibodies act by coating bacteria to enhance phagocytosis and bacterial killing and/or preventing attachment to host cells. In particular, serum IgG and IgA-ASC that target *Shigella* lipopolysaccharide (LPS) have been shown to correlate with protection [3,9,10,18,19].

The role of cell-mediated immunity (CMI) in protection from *Shigella* infections is largely unknown. Elevated levels of IFN- γ and other T-cell-derived cytokines have been proposed to play a role in control and clearance of *Shigella* infections [20–28]. This suggests that either cytokines control the infection directly or they are indicative of other T cell effector functions. For instance, the impact of cytotoxic T cells (CTLs), which kill infected host cells, on *Shigella* clearance is not known [4,29].

Overall, the immune response against *Shigella* must be multifaceted to clear an infection that is both intracellular and extracellular. It is likely that in the clearance of a pathogen such as *Shigella*, antibody responses may be important in the extracellular phase while CMI may play a dominant role in the intracellular phase. An antibody-based vaccine must not only eliminate the bacteria from the gut lumen and lamina propria but should also prevent *Shigella* from entering epithelial cells. Clearance of infected epithelial cells requires a CMI response. Thus, common vaccine targets include lipopolysaccharide (LPS) on the bacterial surface as well as components of the bacteria's type III secretion system, such as IpaB and MxiH, which are critical components of the *Shigella* machinery that allows their entry to epithelial cells [2,3]. Having a clear understanding of which immune interactions are necessary and/or sufficient for protection could greatly aid the development of new multiple-target vaccine strategies [3].

To this end, we develop mathematical models of the immune response against *Shigella* in order to better qualitatively and quantitatively determine the effector immune responses that correlate with protection. We capture the primary immunological and bacterial dynamics with systems of ordinary and delay differential equations. Delays are employed to incorporate biological time-scale differences between existing immunity and new immune activation. Thus, in the first few days of an infection, immune protection against *Shigella* is conferred by innate immune cells or existing antibodies elicited by prior infections or vaccines;

later, the presence of *Shigella* antigens elicit robust B and/or T cell responses.

While there has been much ongoing activity in deriving mathematical models of the immune interactions with other diseases (e.g., tuberculosis and influenza [30–35]), to the best of our knowledge, this is the first mathematical model of the immune response against *Shigella*. Furthermore, while other mathematical studies have examined the impact of vaccines on pathogen dynamics ([36,37]), the application to *Shigella* vaccine development is novel.

We focus on *Shigella*'s interactions with the humoral immune response, which consists of antibodies (IgA and IgG, which function predominantly in the gut lumen and lamina propria, respectively), ASC, and B_M cells. We incorporate an innate immune cell compartment in which *Shigella* is subject to phagocytic killing but escapes antibody action. Notably, our model does not include cell-mediated immunity components such as CTLs that might eradicate *Shigella* bacteria inside host epithelial cells, as T cell activity against *Shigella* remains largely undefined. Using the model, we examine infection dynamics both in the presence and absence of an assumed *Shigella* vaccine directed against *Shigella* outer membrane components, such as lipopolysaccharide (LPS), that are displayed throughout an infection. We investigate whether LPS-directed antibodies are sufficient to prevent a severe *Shigella* infection. The model incorporates both mucosal (IgA) and systemic (IgG) immune responses, and we compare which is most effective. We also focus in on *Shigella*'s ability to infect host epithelial cells and ask if antibodies directed against epithelial entry are necessary components of a successful *Shigella* vaccine.

The structure of this paper is as follows: we first derive the model and explain the underlying biological dynamics that it captures. In the Analysis section, we identify the equilibria, including disease-free and vaccinated states, and evaluate their stability. In the Dynamics section, we present numerical simulations of the model to determine immune and bacterial dynamics before and after vaccination, to quantify the number of anti-LPS antibodies required for immune protection, and to explore the potential effectiveness of epithelial entry targeting. In the Parameters section, we alternately vary certain parameters to deduce their impact on model results (while leaving more rigorous sensitivity analysis to future studies) and we identify key factors that potentially correlate with *Shigella* immunity. Finally, we summarize our results and discuss their implications on the *Shigella* vaccine development process.

In the broader sense, this paper lays the foundation for determining *Shigella*'s immunological correlates of protection by developing mathematical models of the immune response against *Shigella*. Model results improve our understanding of the immune response elicited against *Shigella*, suggest alternative approaches to future vaccine design, and take the first steps in forecasting the success of their implementation.

Methods

We write a system of differential equations to capture bacterial and immune dynamics and focus on humoral immune components that can potentially be elicited through vaccination. Bacterial pathogenesis and the reaction diagram corresponding to the model are given in Figure 1. A primary goal of vaccination is the establishment of B_M populations that maintain antibody and ASC (plasma cell) populations; thus, all three serve as model variables. Furthermore, we distinguish between IgA and IgG at both the antibody and cellular level in order to parse potential differences between mucosal (IgA) and systemic (IgG) immune responses. We

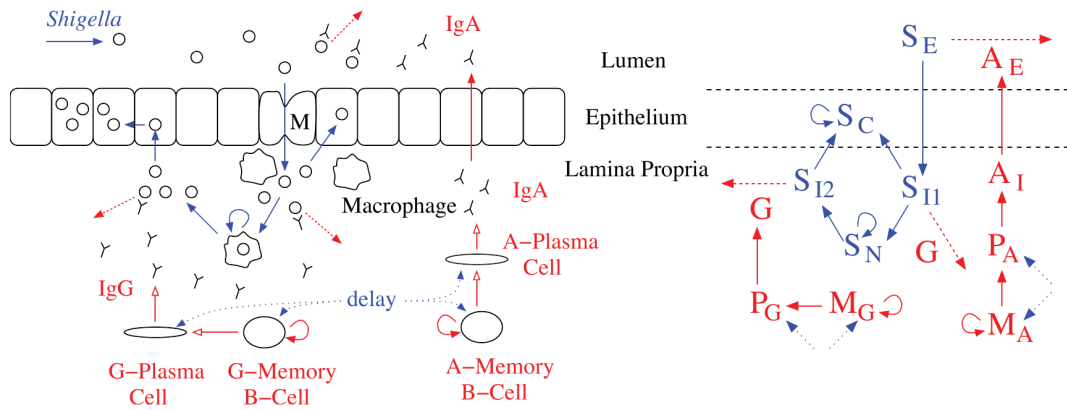


Figure 1. Simplified schematic of the predicted interactions of *Shigella* and the host in the gut. We translate bacterial pathogenesis (blue) plus antibody and B cell dynamics (red) seen in vivo (left) to mathematical reactions (right). The most severe symptoms result when *Shigella* escapes the humoral immune response by infecting epithelial cells. Prior to this, *Shigella* can be removed by antibodies (luminal IgA or lamina propria IgG targeting LPS in *Shigella*'s outer membrane) or engulfed by macrophages (from which it escapes or is destroyed). Delay in creation of new B cells from naive cells during infection is included in the model. Abbreviations: *S*: *Shigella*, *A*: IgA, *G*: IgG, *M*: B_M , *P*: ASC, *I*: in Lamina Propria, *E*: Luminal, *C*: Epithelial, *N* Engulfed.
doi:10.1371/journal.pone.0059465.g001

do not include cytotoxic T cells, which could play a key role in controlling wild-type *Shigella* once they have invaded host epithelial cells, macrophages, and other cells, since a role for this effector CMI activity in fighting infection remains to be well characterized [3].

In our model, we incorporate delays into mathematical terms for the creation of new B_M and new plasma cells from naive cells during an infection. This captures the day-or-longer time frame from naive activation to effector/memory functionality in which naive B cells proliferate and differentiate to form new cell types. We also assume a 3.5-day delay from the start of a *Shigella* infection to the initialization of a new immune response; in this time window, only previously established antibodies and B cell dynamics can target the bacterial population.

Our model consists of a system of ordinary and delay differential equations that tracks bacterial populations in multiple spatial compartments as well as the immune response composed of *Shigella*-specific IgA and IgG B_M , plasma cells, and antibodies. At the start of infection, *Shigella* takes advantage of a natural activity of host M cells, which shuttle material from the lumen across the epithelium to innate immune cells such as macrophages that wait in the lamina propria to engulf *Shigella* and destroy it. *Shigella* travels from the lumen, where it is denoted S_E , into the lamina propria (S_{I1}) at rate μ_E , where it either is engulfed by macrophages (becoming S_N) at rate μ_{NI} or escapes and can enter epithelial host cells (becoming S_C) at rate μ_{I1} . Most bacteria are typically destroyed inside macrophages; however, engulfed *Shigella* can avoid destruction and proliferate at rate σ_N inside macrophages, where *Shigella* is safe from antibody targeting, and then escape back out into the lamina propria (becoming S_{I2}) at rate μ_N . From there, we assume *Shigella* is sufficiently distant from the M cells and other macrophages to have no likelihood of re-engulfment; it instead can infect epithelial cells at rate μ_{I2} and transition to the S_C population. We will discuss later how altering this no re-engulfment assumption impacts infection dynamics.

Once within the epithelium, *Shigella* proliferates at rate σ_C and has the ability to migrate directly between epithelial cells without reentering the lamina propria; this stage causes substantial epithelial cell destruction, which is responsible for inducing the most severe symptoms of shigellosis. To keep our first attempt at

modeling *Shigella* infection relatively simple, we elected not to include in the model cell-to-cell spread or epithelial cell destruction directly (this is left to a future model) but rather assume epithelial stress correlates with significant epithelial invasion and hence high values for S_C . In order to prevent permanently recurring infections, we assume bacterial migration from the epithelium (S_C) to the lumen (S_E) does not occur; thus, we only examine within-host dynamics, and the likelihood of person-to-person transmission along a fecal-oral route cannot be predicted with this model. By similar reasoning, we do not include the small likelihood of luminal *Shigella* proliferating before entering the lamina propria in order to avoid mathematically establishing a luminal *Shigella* population that persistently spawns new infections.

The equations governing the bacterial dynamics are as follows:

$$\frac{dS_E}{dt} = -\delta_{SE}S_E - \mu_E S_E - \alpha(A_E)S_E \quad (1)$$

$$\frac{dS_{I1}}{dt} = -\delta_{SI}S_{I1} + \mu_E S_E - \mu_{NI}S_{I1} - \mu_{I1}S_{I1} - \gamma(G)S_{I1} \quad (2)$$

$$\frac{dS_N}{dt} = \sigma_N S_N - \delta_{SN}S_N + \mu_{NI}S_{I1} - \mu_N S_N \quad (3)$$

$$\frac{dS_{I2}}{dt} = -\delta_{SI}S_{I2} + \mu_N S_N - \mu_{I2}S_{I2} - \gamma(G)S_{I2} \quad (4)$$

$$\frac{dS_C}{dt} = \sigma_C S_C - \delta_{SC}S_C + \mu_{I2}S_{I2} + \mu_{I1}S_{I1} \quad (5)$$

Here, the death rates (δ terms) incorporate *Shigella* death due to macrophage activity or other causes; *Shigella* removal via antibody is modeled separately. A_E and G are luminal IgA and lamina propria IgG, respectively, and their dynamics are governed by the immune response equations below. We assume these antibodies

recognize and bind specifically to *Shigella* outer membrane components such as LPS, which is constantly displayed and available for antibody targeting whenever *Shigella* resides in the lamina propria or lumen. When sufficient numbers (n_E or n_I , respectively) of IgA or IgG bind to a *Shigella* bacterium, the bacterium is removed or destroyed. We assume the null model of linear interaction terms as the functional forms capturing bacterial removal via antibodies; that is, $\alpha(A_E) = \alpha A_E$ and $\gamma(G) = \gamma G$. These terms could become more complex in future work if that is needed to better match with experimental or clinical dynamics.

The humoral immune response to *Shigella* consists of IgG-type B_M (denoted M_G), IgG-secreting plasma cells (P_G), and the IgG antibodies themselves (G), in the lamina propria. IgA antibodies are formed in the lamina propria from IgA-secreting plasma cells (P_A), which are often derived from IgA-type B_M cells (M_A); IgA (A_I) then reaches the lumen by crossing the epithelial barrier (via interactions with the pIgR receptors or the paracellular pathway, becoming A_E), where IgA functions primarily. Antibody secretion by each plasma cell occurs constantly at rate β_A or β_G , regardless of infection status, just as memory cells differentiate to form ξ plasma cells at a low rate ϕ_1 even without an infection currently occurring. However, the presence of bacteria within the lamina propria stimulates further B_M differentiation into plasma cells (ϕ_{2A} and ϕ_{2G} functions) while also stimulating naive B cells to create new plasma cells (λ_{PA} and λ_{PG} functions) and new B_M cells (λ_{MA} and λ_{MG} functions). In the model, the latter four terms incorporate a time delay, τ , to allow time for the window between naive-cell activation and differentiated-cell functionality, as described earlier. In the absence of an infection, B_M cell generation, death, and differentiation rates must balance to establish a nontrivial (nonzero) memory population that neither expand nor shrink over time. To prevent the system from becoming neutrally stable when this occurs, we assume B_M follow logistic growth dynamics.

Summarizing these immune dynamics are the following model equations:

$$\frac{dA_E}{dt} = -\delta_{AE}A_E + \omega A_I - n_E \alpha(A_E)S_E \tag{6}$$

$$\frac{dA_I}{dt} = -\delta_{AI}A_I - \omega A_I + \beta_A P_A \tag{7}$$

$$\frac{dG}{dt} = -\delta_G G + \beta_G P_G - n_I \gamma(G)(S_{I1} + S_{I2}) \tag{8}$$

$$\begin{aligned} \frac{dP_A}{dt} = & -\delta_{PA}P_A + \lambda_{PA}(S_{I1}(t-\tau) + S_{I2}(t-\tau)) \\ & + \xi \phi_{2A}(S_{I1} + S_{I2})M_A + \phi_1 M_A \end{aligned} \tag{9}$$

$$\begin{aligned} \frac{dP_G}{dt} = & -\delta_{PG}P_G + \lambda_{PG}(S_{I1}(t-\tau) + S_{I2}(t-\tau)) \\ & + \xi \phi_{2G}(S_{I1} + S_{I2})M_G + \phi_1 M_G \end{aligned} \tag{10}$$

$$\begin{aligned} \frac{dM_A}{dt} = & \rho \left(1 - \frac{M_A}{K_A}\right) M_A - \phi_1 M_A + \lambda_{MA}(S_{I1}(t-\tau) \\ & + S_{I2}(t-\tau)) - \phi_{2A}(S_{I1} + S_{I2})M_A \end{aligned} \tag{11}$$

$$\begin{aligned} \frac{dM_G}{dt} = & \rho \left(1 - \frac{M_G}{K_G}\right) M_G - \phi_1 M_G + \lambda_{MG}(S_{I1}(t-\tau) \\ & + S_{I2}(t-\tau)) - \phi_{2G}(S_{I1} + S_{I2})M_G. \end{aligned} \tag{12}$$

Here the functional forms are again assumed to be linear. We analyze the coupled bacterial and immune equations both analytically and numerically to discern the behavior of the model under different disease conditions. Whenever possible, parameter values have been chosen *a priori* from empirically realistic values found in the literature; they are summarized in Table 1. No parameters have been fitted.

Results

Analysis

Equilibrium analysis elucidates model dynamics between infections. Prior to a primary *Shigella* infection, all variables lie at a trivial equilibrium where no *Shigella* bacteria or immune components specific for *Shigella* yet exist. (The trivial equilibrium disallows potential cross-reactivity with pre-existing antibodies created in response to a different bacterial infection. Inclusion of these must be done externally to the model via initial conditions.) A *Shigella* infection is cleared unless the disease is so acutely severe that it kills the host; however, a B_M population specific for the bacteria remains indefinitely and supports ongoing plasma cell and antibody creation. The model captures this behavior with its disease-free equilibria that have nonzero numbers for antibodies, plasma cells, and B_M while simultaneously having no *Shigella* bacteria in any spatial compartment. Three disease-free equilibria exist for the model: one with mucosal (IgA-type) but not systemic (IgG-type) immunity, one with systemic but not mucosal immunity, and a joint equilibrium with both. The values of the model variables at equilibrium are given in Table 2; these are evaluated at the parameter values in Table 1.

Importantly, there is no completely nontrivial equilibrium of the model, which is consistent with the fact that a *Shigella* infection is never persistent nor chronically latent. If, however, macrophage re-engulfment of *Shigella* in the lamina propria is allowed—that is, if S_{I1} and S_{I2} are combined into S_I with $\mu_{I1} = \mu_{I2} = \mu_I$ —then a persistently infected macrophage population develops that continually seeds the *Shigella* infection and prevents bacterial clearance (not shown). This chronic state is not observed biologically; hence, macrophage re-engulfment is not allowed in the model and the *Shigella* populations in the lamina propria are separate.

Stability of the trivial and disease-free equilibria can be determined by examining the eigenvalues of the Jacobian matrix for our system of differential equations at the equilibria. Since there is no truly nontrivial equilibrium and hence the *Shigella* populations are zero at all equilibria, we examine the stability of the reduced system with $S_E = S_{I1} = S_N = S_{I2} = S_C = 0$. For a generic equilibrium with B_M numbers M_A^* and M_G^* , the Jacobian matrix for this disease-free system is

Table 1. Parameter Values Used In Simulations.

Param	Value Used	Description	Reference or Note
σ_N	0.6/d	<i>Shigella</i> reproduction rate in innate immune cells	high but brief [44]
σ_C	0.1/d	<i>Shigella</i> reproduction rate in epithelial cells	high [45,46] (smaller for numerical stability w/o CTLs)
δ_{SE}	0.0001/d	Natural death rate of <i>Shigella</i> in lumen	minimal
δ_{SI}	0.0001/d	Natural death rate of <i>Shigella</i> in lamina propria	minimal
δ_{SN}	0.2/d	Death rate of <i>Shigella</i> in macrophages	$1 - \mu_N$
δ_{SC}	0.0001/d	Natural death rate of <i>Shigella</i> in epithelium	minimal
δ_{AE}	0.2/d	Natural decay/removal rate of IgA in lumen	3.5 d hl (from δ_G)
δ_{AI}	0.2/d	Natural decay/removal rate of IgA in lamina propria	3.5 d hl (from δ_G)
δ_G	0.2/d	Natural decay/removal rate of IgG in lamina propria	3.5 d hl (18 d hl [42]-localiz.)
δ_{PA}	0.2/d	Natural death rate of IgA-plasma cells	3 d hl (early pc) [42,47,48]
δ_{PG}	0.2/d	Natural death rate of IgG-plasma cells	3 d hl (early pc) [42,47,48]
δ_{MA}	0.03/d	M_I Natural death rate of IgA-B	3 wk hl [49]
δ_{MG}	0.03/d	M_I Natural death rate of IgG-B	3 wk hl [49]
μ_E	0.5/d	Migration rate of <i>Shigella</i> from lumen to lamina propria	low (0.0029% of 10^8 bact/mL) in first 2 h [50]
μ_{I1}	0.05/d	Migration rate of never-engulfed <i>Shigella</i> from lamina propria to epithelium	
μ_{I2}	0.05/d	Migration rate of once-engulfed <i>Shigella</i> from lamina propria to epithelium	
μ_{NI}	0.8/d	Rate <i>Shigella</i> in lamina propria are engulfed by macrophages	fast
μ_N	0.8/d	Rate <i>Shigella</i> escape out of macrophages into lamina propria	fast (macs apoptose in 8 h) [44]
ω	0.05/d	Migration rate of IgA from lamina propria to lumen	20% of total IgA to lumen
n_E	8000 Ab/bact	Number of IgA that neutralize a luminal bacterium	(from n_I)
n_I	8000 Ab/bact	Number of IgG that neutralize a lamina propria bacterium	[51]
β_A	10^9 /d	Production rate of IgA by IgA-plasma cells	10^5 /sec [42,52–55]
β_G	10^9 /d	Production rate of IgG by IgG-plasma cells	10^5 /sec [42,52–55]
ϕ_1	0.01 pc/mc/d	Antigen-independent differentiation rate of B_M into plasma cells	
ρ	0.04/d	M_I Antigen-independent cycling rate of B	
ξ	2000 pc/mc	Number of plasma cells generated by proliferating M_I antigen-activated B	
α	10^{-14} /Ab/d	Rate antibodies neutralize <i>Shigella</i> in lumen	
γ	10^{-14} /Ab/d	Rate antibodies neutralize <i>Shigella</i> in lamina propria	
ϕ_{2A}	0.01/bact/d	M_I Antigen-dependent rate function for IgA-B differentiation into plasma cells	
ϕ_{2G}	0.01/bact/d	M_I Antigen-dependent rate function for IgG-B differentiation into plasma cells	
k_A	1000 mc	IgA- B_M carrying capacity	
k_G	1000 mc	IgG- B_M carrying capacity	
λ_{PA}	0.1 pc/bact/d	Creation rate of new IgA-plasma cells from naive B cells	
λ_{PG}	0.1 pc/bact/d	Creation rate of new IgG-plasma cells from naive B cells	
λ_{MA}	0.1 pc/bact/d	Creation rate of new IgA- B_M from naive B cells	
λ_{MG}	0.1 pc/bact/d	Creation rate of new IgG- B_M from naive B cells	
τ	1 d	Time delay for new cell creation from naive B cells	
–	3.5 d	Initial delay until naive B cell activation in an infection	

Table 1. Cont.

Param	Value Used	Description	Reference or Note
θ	10^{-11}	Nonmechanistic term governing the effect of IgG targeted at epithelial entry	
$S_E(0)$	1000 bact	Initial number of luminal <i>Shigella</i>	1000 minimum [19,38–40]

Parameter values used in the model are given along with their descriptions. Applicable references or notes are given. Uncited parameters were chosen *a priori* and are not fitted. The initial condition for establishing a (luminal) *Shigella* infection is given. Other initial conditions are taken from the equilibria in Table 2. Abbreviations: d: day, Ab: antibodies, pc: plasma cells, mc: B_M cells, bact: *Shigella* bacterium, hl: half-life.
doi:10.1371/journal.pone.0059465.t001

$$\begin{bmatrix} -\delta_{AE} & \omega & 0 & 0 & 0 & 0 & 0 \\ 0 & -\delta_{AI} - \omega & 0 & \beta_A & 0 & 0 & 0 \\ 0 & 0 & -\delta_G & 0 & \beta_G & 0 & 0 \\ 0 & 0 & 0 & -\delta_{PA} & 0 & \phi_1 & 0 \\ 0 & 0 & 0 & 0 & -\delta_{PG} & 0 & \phi_1 \\ 0 & 0 & 0 & 0 & 0 & -\phi_1 + \rho - \frac{2\rho}{\kappa_A} M_A^* & 0 \\ 0 & 0 & 0 & 0 & 0 & 0 & -\phi_1 + \rho - \frac{2\rho}{\kappa_G} M_G^* \end{bmatrix}$$

and the eigenvalues of the reduced system are

$$-\delta_{AE}, -\delta_{AI} - \omega, -\delta_G, -\delta_{PA}, -\delta_{PG}, \rho - \phi_1 - \frac{2\rho}{\kappa_A} M_A^*, \rho - \phi_1 - \frac{2\rho}{\kappa_G} M_G^*.$$

If the following two stability conditions are satisfied, the eigenvalues are all negative and hence the corresponding equilibrium is stable:

$$M_A^* > \frac{\rho - \phi_1}{2\rho} \kappa_A \text{ and } M_G^* > \frac{\rho - \phi_1}{2\rho} \kappa_G. \quad (13)$$

For our parameters, this means that stability occurs exactly when both M_A^* and M_G^* exceed 375 cells. Therefore, from the parameterized equilibrium values in Table 2, it is apparent that the joint (IgA and IgG) disease-free equilibrium is stable while the trivial equilibrium, IgA-only disease-free equilibrium, and IgG-only disease-free equilibrium are saddle points.

Thus, following a primary *Shigella* infection, the trivial equilibrium is not maintained and some level of permanent immunity is established. If only A-type or G-type immunity is generated initially, another infection could boost the system to the stable joint

Table 2. Equilibrium Values.

	$S_C S_E, S_{I1}, S_N, S_{I2},$	A_E	A_I	G	$P_G P_A,$	$M_G M_A,$
Trivial						
(Pre-Infection)	0 Bacteria	0 Ab	0 Ab	0 Ab	0 Cells	0 Cells
Disease-Free:						
IgA only	0 Bacteria	3.8×10^{10} Ab	1.5×10^{11} Ab	0 Ab	38 Cells,	0 Cells
(Post-Infection)						
Disease-Free:						
IgG only	0 Bacteria	0 Ab	0 Ab	1.9×10^{11} Ab	0 Cells, 38 Cells	0 Cells, 750 Cells
(Post-Infection)						
Disease-Free:						
IgA and IgG	0 Bacteria	3.8×10^{10} Ab	1.5×10^{11} Ab	1.9×10^{11} Ab	38 Cells	750 Cells
(Post-Infection)						
Nontrivial						
(Chronic Infection) none						
Nonzero Terms:						
	$A_E = \frac{\omega \beta_A \phi_1 \kappa_A (\rho - \phi_1)}{\rho \delta_{PA} (\delta_{AI} + \omega) \delta_{AE}}$		$P_A = \frac{\phi_1 \kappa_A (\rho - \phi_1)}{\rho \delta_{PA}}$		$M_A = \frac{\kappa_A (\rho - \phi_1)}{\rho}$	
	$A_I = \frac{\beta_A \phi_1 \kappa_A (\rho - \phi_1)}{\rho \delta_{PA} (\delta_{AI} + \omega)}$		$P_G = \frac{\phi_1 \kappa_G (\rho - \phi_1)}{\rho \delta_{PG}}$		$M_G = \frac{\kappa_G (\rho - \phi_1)}{\rho}$	
	$G = \frac{\beta_G \phi_1 \kappa_G (\rho - \phi_1)}{\rho \delta_{PG} \delta_G}$					

Values of model variables at the equilibria are given. The equilibria are evaluated at the parameters in Table 1. Abbreviation: Ab: antibodies, S: *Shigella*, A: IgA, G: IgG, M: B_M, P: ASC, I: in Lamina Propria, E: Luminal, C: Epithelial, N Engulfed.
doi:10.1371/journal.pone.0059465.t002

disease-free immune state. Whether these immune levels are sufficient to confer protective immunity to the host remains to be determined. Nevertheless, the model supports the hypothesis that a vaccine, which perturbs the immune system away from the trivial equilibrium, will establish a persistent nontrivial level of humoral immunity specific for *Shigella*.

Dynamics

We assess the behavior of the mathematical model via numerical simulations. Using a delay differential equation solver in MATLAB, we examine the bacterial and immune dynamics during a *Shigella* infection that occurs either prior to or months after the administration of a vaccine; the action of the vaccine mathematically is to shift the system from the trivial equilibrium to a disease-free equilibrium. Therefore, a primary *Shigella* infection initializes with trivial variable values while a post-vaccine *Shigella* infection starts at a disease-free equilibrium. (We investigate a vaccine that elicits both IgA and IgG, and accordingly the model initializes at the joint IgA-IgG disease-free equilibrium for a post-vaccine infection.) Parameter values are given in Table 1, and their impact is discussed in the Parameters section.

We establish an infection by assuming enough *Shigella* is ingested to introduce a population of 1,000 bacteria into the gut lumen. Since a minimum of 100–1000 *Shigella* bacteria clinically cause disease, this is sufficient to cause infection [19,38–40]. When invading bacteria meet a naive immune system, the dynamics in Figure 2 result. *Shigella* grows and migrates unfettered in the host during the incubation period before sufficient numbers of naive B cells have been stimulated to create ASC and B_M cells that target the infection. We have built a 3.5-day incubation period into the model prior to immune initiation; after this time, a B cell and antibody response is generated that eliminates the bacterial infection. IgA and IgG levels peak roughly 10–21 days after infection and equilibrate after about one month. Plasma cells and B_M cells also reach new homeostatic levels after about a month. Crucially, these levels are consistent with a disease-free equilibrium's nontrivial immune levels rather than with the trivial equilibrium at which the system began. Immune activity clears the *Shigella* infection to below one bacterium in the lumen and lamina propria in 20 days, but bacteria that enter epithelial cells escape humoral immune targeting and grow without restraint. It should be noted that *Shigella*'s infection of the epithelium may be controlled by cytotoxic T cells and thus in reality this epithelial population would be more controlled; however, T cell activity against *Shigella* remains largely undefined; thus we have not included them in the model. As a result, true *Shigella* dynamics in response to both humoral and cell-mediated immune responses are outside the purview of this model. For our purposes, the essential fact shown by the primary infection model is that *Shigella* can survive well in the epithelium and thus a vaccine that effectively protects against shigellosis must prevent most epithelial entry.

Secondary immune responses are elicited when a vaccine is given that elicits LPS-directed IgA and IgG humoral immune responses and shifts the immune system to the joint disease-free equilibrium. After the host system re-equilibrates, 1,000 wild-type *Shigella* bacteria are introduced to the gut. The dynamics of this secondary *Shigella* infection are depicted in Figure 3. A larger absolute immune response, as evidenced by the antibody and B cell peaks, is stimulated by this secondary infection (Figure 3b); this is consistent with the fact that memory cells elicit stronger and more rapid reactions than naive cells. The vaccine decreases the duration of the bacterial infection by nearly half—from 20 days to 11.5 days until complete clearance (Figure 3a). It also lessens the

severity of the infection, as seen by comparing the height of the “lamina propria” and “innate” *Shigella* peaks. (The luminal peak is fixed to 1,000 by initial conditions.) Also noteworthy are the slowed dynamics of the epithelial cell infection, which suggests the host may experience temporarily reduced symptoms resulting from epithelial destruction. Nevertheless, the vaccine does not fully prevent the epithelial infection, which means the host must instead hope that a primary cytotoxic T cell response can clear it.

We next ask if *Shigella*'s infection of epithelial cells could be prevented purely by anti-LPS antibodies if they were available in larger supply (Figure 4). Here, we boost antibody numbers above vaccine levels, for instance via a pre-infection serum injection of antibodies, while B cell numbers remain at levels established by a vaccine. We examine how many IgA and IgG molecules must be present to restrain *Shigella*'s epithelial population to a given day-45 threshold. By day 45, a wild-type *Shigella* infection will have cleared; thus, we assume that if we can control the bacterial population for long enough through antibody responses, other host's immune responses such as CMI (e.g., cytotoxic T cells or production of IFN- γ and other pro-inflammatory cytokines that activate macrophages and enhance their ability to kill intracellular *Shigella*) will be sufficient to clear the infection. In fact, recent publications have begun to show that CMI responses are important. For example, the clearance of a primary *Shigella* infection is impaired in the absence of T cells. Additional studies demonstrated that following reinfection, IL-17A and IL-22 producing T cells are primed by *Shigella* and the IL-17A produced by these cells restricts bacterial growth [41]. Furthermore, elevated levels of IFN- γ have been shown in humans with shigellosis or following administration of candidate attenuated *Shigella* vaccines [20–27].

The maximum tolerable day-45 threshold should be fixed as a number of *Shigella* that can infect the epithelium without the host becoming severely symptomatic; as this value is unknown, we vary the peak number of bacteria allowed and examine the corresponding antibody requirements (Figure 4). From Table 2, we know that in the order of 10^{11} IgA and IgG established via vaccine are sustained at the joint disease-free equilibrium. Yet from Figure 4, it is clear that holding *Shigella* to small numbers requires much higher initial antibody levels; for instance, it takes 10^{16} IgA alone, 10^{16} IgG alone, or 10^{15} IgA and IgG together in the GI tract to keep the *Shigella* epithelial population at day 45 below 100 bacteria. This four-orders-of-magnitude increase in initial antibody levels could be difficult to elicit biologically and may be untenable.

From Figure 4 we can also parse the relative effectiveness of IgA versus IgG. We assume equal rate parameters but different spatial dynamics for IgA and IgG; IgG removes bacteria in the lamina propria while IgA is made in the lamina propria but functions in the lumen. Figure 4b displays horizontal slices through the surface in Figure 4a. The center diagonal shows where equal amounts occur. From Figures 4a and 4b, we see that IgA and IgG are nearly equally effective alone, with IgG being slightly more potent. However, we must examine the details more carefully to discern true differences in antibody efficacy. These figures show the total amount of IgA in comparison with IgG. However, IgA is distributed across two spatial compartments: the lamina propria, where it is formed, and the lumen, where it functions antimicrobially. The amount of IgA in the lumen versus the lamina propria initially is consistent with the ratio from Figure 2, in which 20% of total IgA is present in the lumen at homeostasis. Thus, in Figures 4a and 4b, 20% of the total IgA acts nearly comparably to 100% of IgG, which does not have spatial compartmentalization. This suggests that A-type antibodies may actually be more

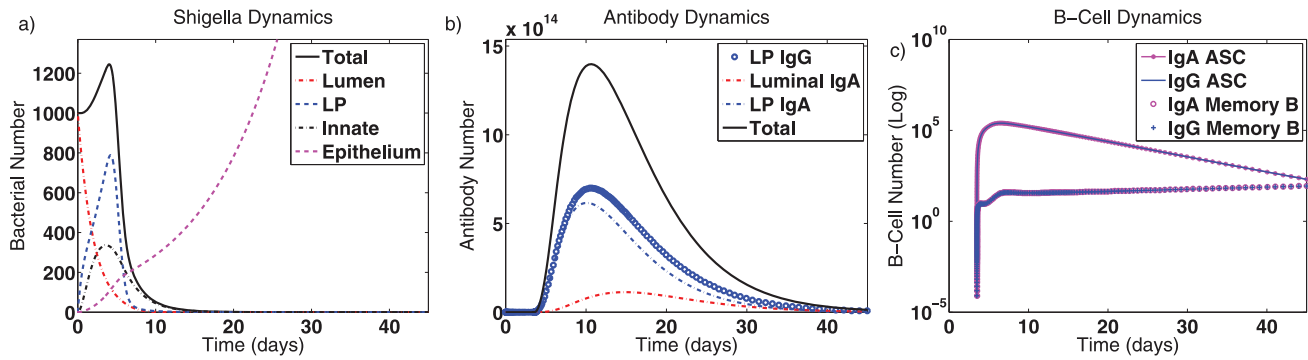


Figure 2. Dynamics of the mathematical model for a primary infection. Here, the model is initialized at a fully naive state (the trivial equilibrium) with 1,000 luminal *Shigella* bacteria. Resulting model dynamics over 45 days are displayed. (a) Bacterial dynamics are shown in the lumen, in the lamina propria (LP, which combines population numbers before and after macrophage engulfment), inside innate immune cells (macrophages) during engulfment, and in epithelial cells. (b) Antibody dynamics are shown for lamina propria IgG, lamina propria IgA, and luminal IgA. Total antibody levels are also given. (c) ASC and B_M dynamics are given on a log scale. These are separated into IgA- versus IgG-type cells. The populations equilibrate to the values shown in Table 2. doi:10.1371/journal.pone.0059465.g002

effective than G-type on a per-molecule basis. We check this by repeating the simulation done to create Figures 4a and 4b but instead requiring that 100% of the total IgA migrates to the lumen. Figure 4c shows that this has little overall effect, but careful examination of the intercepts shows that IgA is now slightly more potent than IgG. Thus, if only one type of antibody response can be elicited by a vaccine, either a mucosal (IgA) or a systemic (IgG) response will be about equally effective. An IgA-only response may require more total antibodies to sustain a sufficient luminal concentration, but each individual IgA molecule is indicated to be slightly more efficacious. If both IgA and IgG can be elicited instead of only one, there is an order-of-magnitude drop in the total amount of antibody needed for protection.

Another option to improve the efficacy of the vaccine's control on the epithelial invasion is to modify the vaccine targets. We have shown that large amounts of IgA and IgG must be present for a vaccine targeting *Shigella* outer membrane components such as LPS to be effective. What if we additionally include an antibody population capable of specifically targeting epithelial entry? To examine this question, we alter the model to allow IgG to nonmechanistically modulate the rate at which in the lamina propria *Shigella* enters epithelial cells. Equation 5 becomes

$$\frac{dS_C}{dt} = \sigma_C S_C - \delta_{S_C} S_C + \frac{\mu_{I_2}}{\theta_{G+1}} S_{I_2} + \frac{\mu_{I_1}}{\theta_{G+1}} S_{I_1}. \quad (14)$$

The inclusion of epithelial targeting by antibodies has the desired effect of almost entirely preventing bacterial invasion of epithelial cells, as can be seen in Figure 5. Although the epithelial population is fractionally higher than zero, this negligible bacterial population that succeeds in circumventing these tightened immune constraints will likely be eliminated through other host defenses. It should be noted that in this altered model we imperfectly assume that the same IgG population can target both LPS and epithelial entry; a future, mechanistic model will separate these populations. However, this simple, nonmechanistic approach demonstrates that targeting epithelial entry can be a successful strategy in theory and is worth pursuing in more detail. Future work must also take into account other important issues, such as potentially brief availability of epithelial entry proteins.

Parameters

The model parameters have been chosen from the literature whenever possible (Table 1). No parameters have been fitted.

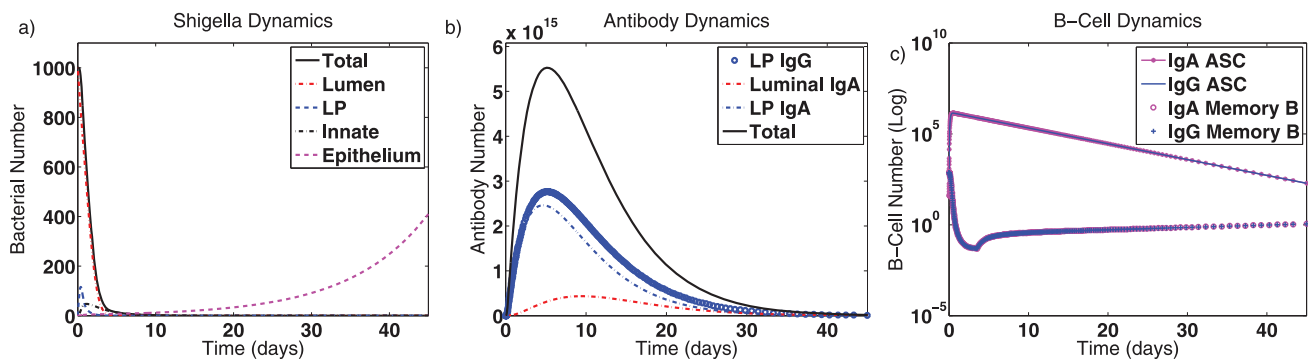


Figure 3. Dynamics of the mathematical model for a secondary or post-vaccine *Shigella* infection. Mathematically, a vaccine (which targets *Shigella* outer membrane components such as LPS) shifts the system to its nontrivial immune equilibrium. Here, the model is initialized at the joint IgA-IgG disease-free equilibrium with 1,000 luminal *Shigella* bacteria. The duration and severity of infection decrease and the immune response is boosted in comparison with a primary infection (Figure 2). Abbreviations: LP: lamina propria, ASC: antibody-secreting cells. doi:10.1371/journal.pone.0059465.g003

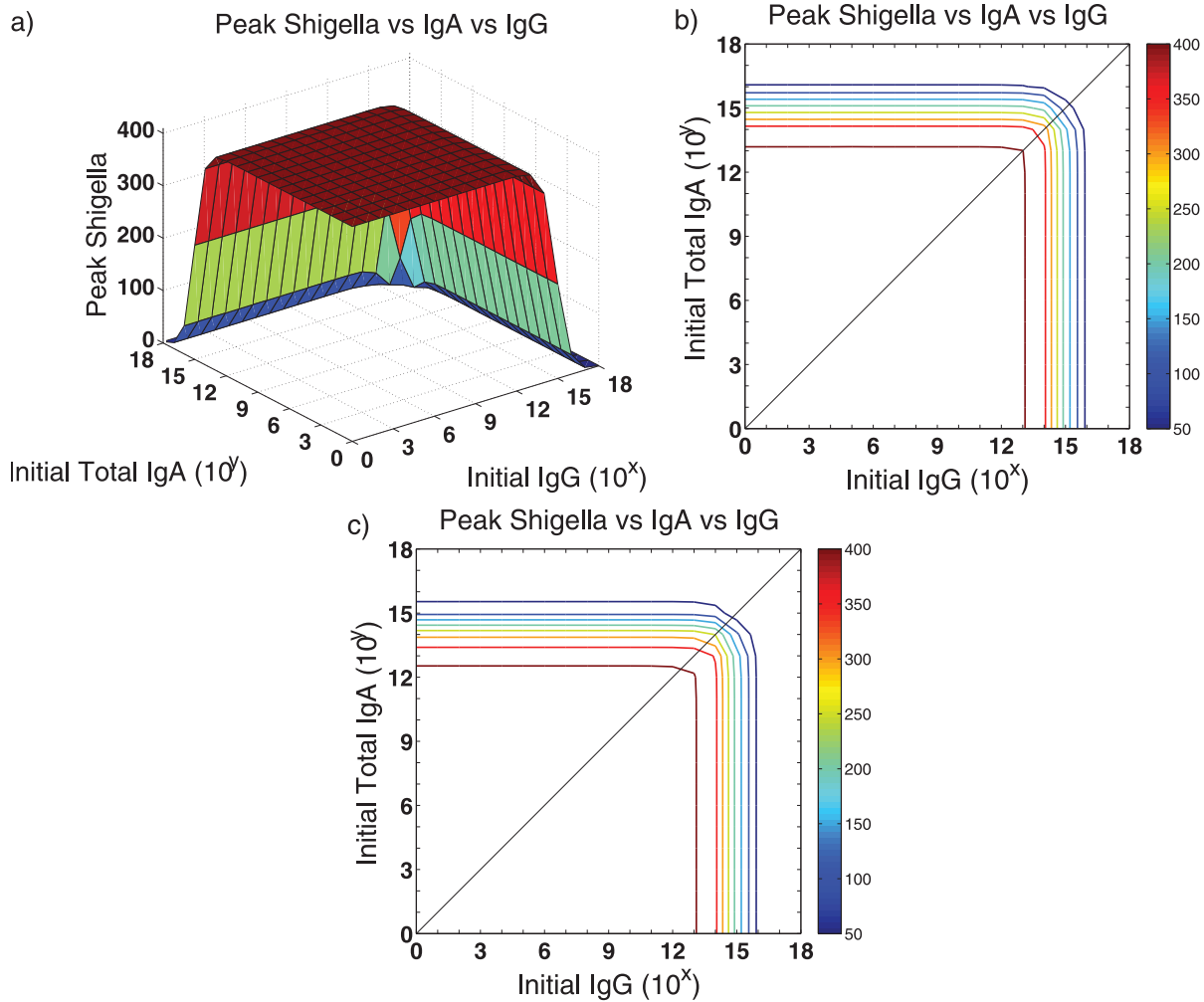


Figure 4. The number of antibodies needed to control an epithelial *Shigella* infection is shown. We examine the quantity of IgA and/or IgG antibodies that must be present prior to a post-vaccine or secondary infection to sufficiently contain the infection. We initialize the model with IgG and/or total IgA numbers each varying from 10^0 through 10^{18} antibodies and display the peak number of non-luminal *Shigella* organisms by day 45. The unboosted model's post-vaccine equilibrium of 10^{11} antibodies is four orders-of-magnitude less than what is necessary to keep the *Shigella* epithelial population below 100 bacteria. (a,b) Figure b displays horizontal slices through the surface in a. With the parameters in Table 1, 20% of total IgA reaches the lumen, where it functions; thus, we fix the ratio of initial luminal IgA to total IgA at 0.2. Comparing x- and y-intercepts for each contour line reveals that with only 20% of IgA functional, slightly more total IgA alone is needed to be as effective as IgG alone. (c) We change the ratio of initial luminal IgA to total IgA to 1, and thus 100% of total IgA reaches the lumen and is functional. The surface that was sliced to create c is not shown. The resulting intercepts for peak day-45 *Shigella* numbers reveal that with the number of functional IgA identical to the number of functional IgG, IgA is slightly more effective than IgG. doi:10.1371/journal.pone.0059465.g004

While a detailed search of parameter space is outside the scope of this current study, we explore the role of individual model parameters on the model dynamics by conducting further simulations in which we vary a single parameter while leaving the rest at the values in Table 1. We monitor the post-vaccine dynamics over 45 days. For any chosen parameter range, we measure and plot.

1. The magnitude and timing of peak total antibody numbers.
2. The magnitude and timing of the peaks in *Shigella* numbers in each spatial compartment.
3. The time of extinction of *Shigella* in non-epithelial compartments, which we define as having less than one *Shigella* bacterium total in the lumen, lamina propria, or engulfed populations.

4. The time until antibody decays to 10% of its peak value.

The biological values of many of these quantities are unknown (Table 1). The goal of this study is to determine the degree of dependence of the predicted outcomes on the underlying parameters. We primarily focus on varying parameters about whose values we are most uncertain in the context of shigellosis. These are the antibody decay rates (δ_{AE} , δ_{AI} , and δ_G), the rate antibodies neutralize *Shigella* (α and γ), the B_M carrying capacities (κ_A and κ_G), the rate B_M differentiate into plasma cells upon antigenic stimulation (ϕ_{2A} and ϕ_{2G}), the number of plasma cells generated by proliferating antigen-activated B cells (ζ), the rate that plasma cells are generated from antigen-activated B_M cells (λ_{PA} , λ_{PG} , λ_{MA} , λ_{MG}), and the delay terms (τ and the primary infection immune delay). Results of these simulations are shown in Figures 6, 7, 8.

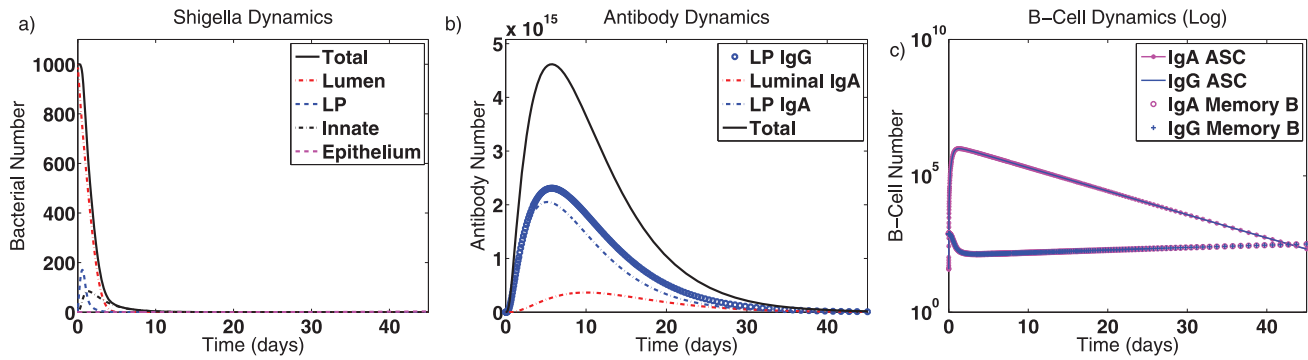


Figure 5. Bacterial and immune dynamics when the model includes antibody targeting of epithelial entry. If the model allows for IgG to nonmechanistically modulate the rate at which lamina propria (LP) *Shigella* enters epithelial cells, these post-vaccine dynamics result. Notably, the epithelial bacterial population is restricted to nearly zero levels. doi:10.1371/journal.pone.0059465.g005

Antibody half-lives have been measured clinically in humans [42]; yet, survival times for antibodies present in the lamina propria may be lower due to time spent localizing to the lamina propria, transcytosis, washout, and other factors. To better understand how antibody survivorship times affect immune and bacterial dynamics, we vary the antibody decay rates (δ_{AE} , δ_{AI} , and δ_G), which we set to be equal to one another, from 0.01/d to 0.3/d. In Figure 6a, we plot the magnitude of the total post-vaccine antibody peak, which sums lamina propria IgG, lamina propria IgA, and luminal IgA. As the natural antibody death rate increases, the peak number of antibodies decreases because the time window over which antibodies present at the peak were created is broader. Figure 6b gives the time at which the antibody peak occurs as well as the time at which only 10% of the peak remains following the infection. Since we limit the time frame to 45 days, the total antibody population never decays to 10% of the peak for small antibody death rates. Comparing these figures, we see that smaller antibody peaks require less time to be reached. Despite the changing antibody peaks, the bacterial peaks do not vary much with the antibody death rates, as seen in Figure 6c, wherein we plot peak *Shigella* numbers in the lumen (L), lamina propria (LP), epithelium (E) or engulfed in innate immune cells (I). In Figure 6d, we plot *Shigella* peak times, which also are independent of this parameter. However, we also plot the time at which the total *Shigella* population in the lumen, lamina propria, and engulfed in innate cells drops below one bacterium, corresponding to *Shigella* extinction in non-epithelial compartments. This extinction time does increase with antibody death rates, likely because the amount of antibody capable of removing bacteria decreases.

We next vary the rate that antibodies neutralize *Shigella* in the lumen and lamina propria (α and γ) from 10^{-25} to 10^{-10} /antibody/day. Our model value of 10^{-14} /Ab/day was chosen for being the largest neutralization rate for which a non-epithelial *Shigella* infection takes at least a day to peak in simulations; it was not chosen as an optimal value that fits more biologically stringent *Shigella* peak behaviors. By varying the value, we see that higher neutralization rates correspond to faster, and thus lower magnitude, antibody peaks (Figures 6e–f). Only for smaller antibody peaks do antibody levels decay to 10% of the peak within 45 days. Little change in peak antibody numbers occurs for a neutralization rate lower than 10^{-19} /Ab/day, which suggests that this is a lower bound on antibody effectiveness. This is confirmed by examining the *Shigella* peak magnitudes (Figure 6g) and times (Figure 6h), which are identical for all neutralization rates below about 10^{-19} /

Ab/day. However, higher neutralization rates lower the peak bacterial load nonlinearly and drive non-epithelial *Shigella* infections to extinction within 0–3 weeks. The epithelial peak also never reaches above 100 bacteria at day 45 for naturalization rates larger than 10^{-13} /Ab/day (Figure 6g); however, such rates lead to the nearly immediate elimination of the *Shigella* infection (Figure 6h) and thus may not be biologically feasible. Whether increasing the neutralization ability of individual antibodies is possible and effective in clinical parameter ranges should be explored in more detail with future modeling.

Since the number of antigen-specific B_M cells needed to confer immunity to *Shigella* is unknown and likely can vary with antigen targets, we vary the carrying capacities (i.e., the maximum sustainable cell numbers in the absence of infection) for IgA- and IgG- B_M cells (κ_A and κ_G) from 10 to 10^6 cells in Figures 6i–l. Increases in the carrying capacities induce roughly the same order-of-magnitude increase in the peak number of total antibodies but does not much affect the timing of the peak or the time at which all but 10% of the peak antibody remains (Figures 6i–j). Interestingly, the carrying capacity for *Shigella*-directed B_M cells does substantially impact the amount of *Shigella* present in the epithelium (Figure 6k). If 10^4 or more *Shigella*-specific IgA- and IgG- B_M cells can be sustained, the peak number of *Shigella* in a post-vaccine infection at day 45 remains below 100 bacteria (Figure 6k). This is due in part to the resulting order-of-magnitude increase in both initial (disease-free equilibria) and peak antibody numbers when the carrying capacities are changed from 1,000 cells to 10,000 cells. However, Figure 4 suggests the presence of 10^{12} total antibodies prior to infection would still not be sufficient to confer protection; this figure assumes a pre-infection boost of antibodies above vaccine levels (via a serum injection of antibodies, for instance) without a corresponding increase in B_M cells or other immunity. This makes clear that an antibody boost alone is not sufficient for immune protection. However, an antibody increase resulting from an underlying boost in B_M cells can confer protection if high enough B_M cells numbers are reached, perhaps because higher antibody levels can then be sustained for longer times. Importantly, from Figure 6k, we see that altering the B_M carrying capacity can improve the effectiveness of a vaccine enough that a purely anti-LPS *Shigella* vaccine could be sufficient to confer immunity. This suggests that anti-LPS B_M cells could serve as correlates of immunity and should be a key focus of future work in parallel with explorations of epithelial entry protein targeting.

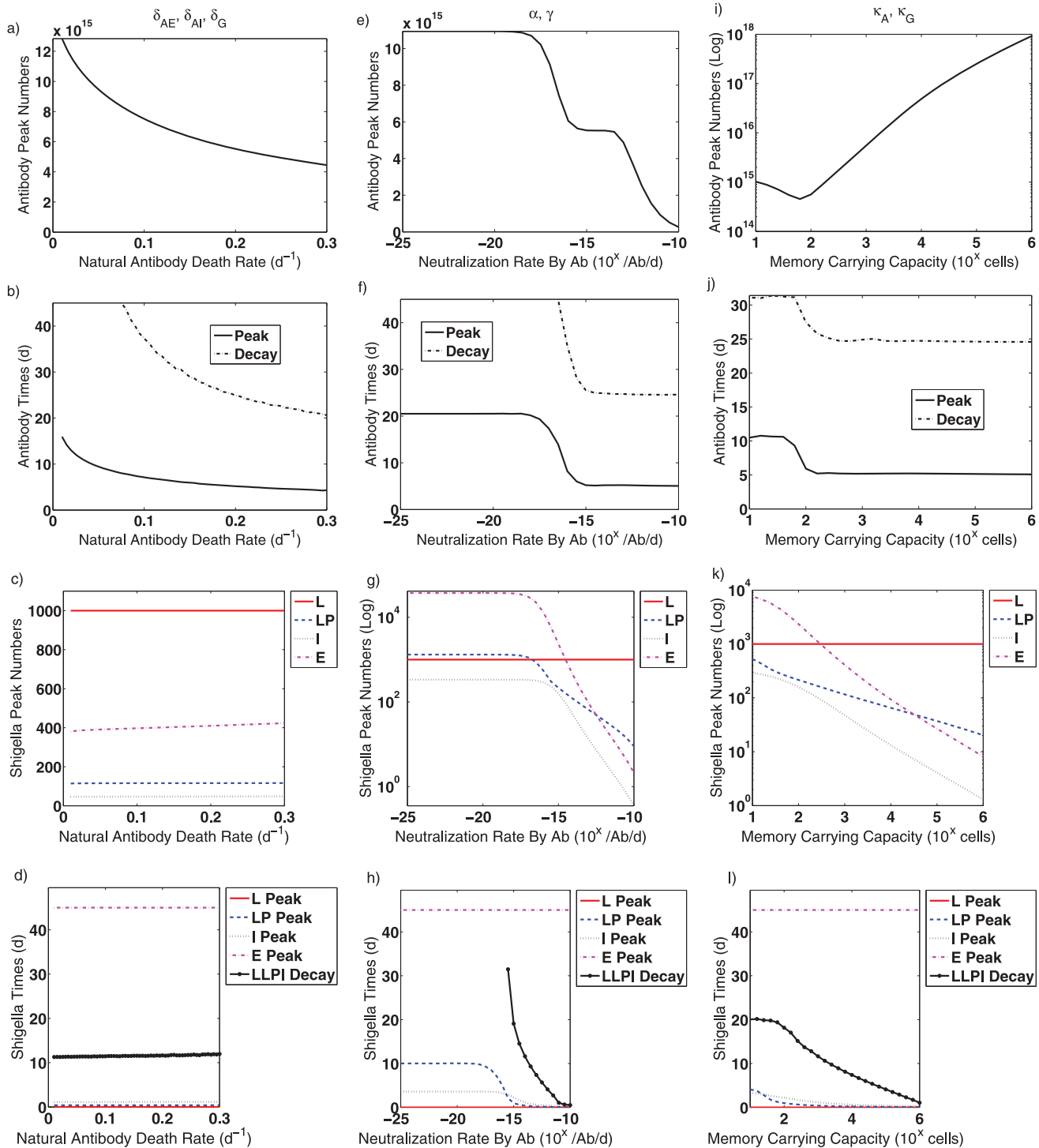


Figure 6. Effects of various parameters on post-vaccine dynamics are evaluated. Only one parameter type varies in each figure; other parameters are fixed to the values given in Table 1. (a–d) The natural antibody death rates (δ_{AE} , δ_{AI} , and δ_G) are varied together from 0.01 to 0.3/d. (e–f) The rates that a *Shigella* bacterium is neutralized by antibody (α for IgA and γ for IgG) are varied together from 10^{-25} to $10^{-10}/\text{Ab/d}$. (i–l) The B_M carrying capacities (κ_A and κ_G) are varied from 1 to 10^6 cells. The following results are tracked for each parameter: (a,e,f) the peak number of total antibody (lamina propria IgG plus lamina propria and luminal IgA), (b,f,j) the timing of the antibody peak, (c,g,k) the peak number of *Shigella* in the lumen (L), in the lamina propria (LP), engulfed in innate immune cells (I), and in the epithelium (E), (d,h,l) the timing of the *Shigella* peak in the aforementioned compartments as well as the time at which the total number of non-epithelial *Shigella* drops below one bacterium (LLPI Decay). Abbreviations: Ab: antibodies, d: day, L: lumen, LP: lamina propria, I: engulfed in innate immune cells, E: epithelium, Log: logarithmic scale, 10^x : the number on the x-axis should be used as the exponent of 10 to obtain the true value. doi:10.1371/journal.pone.0059465.g006

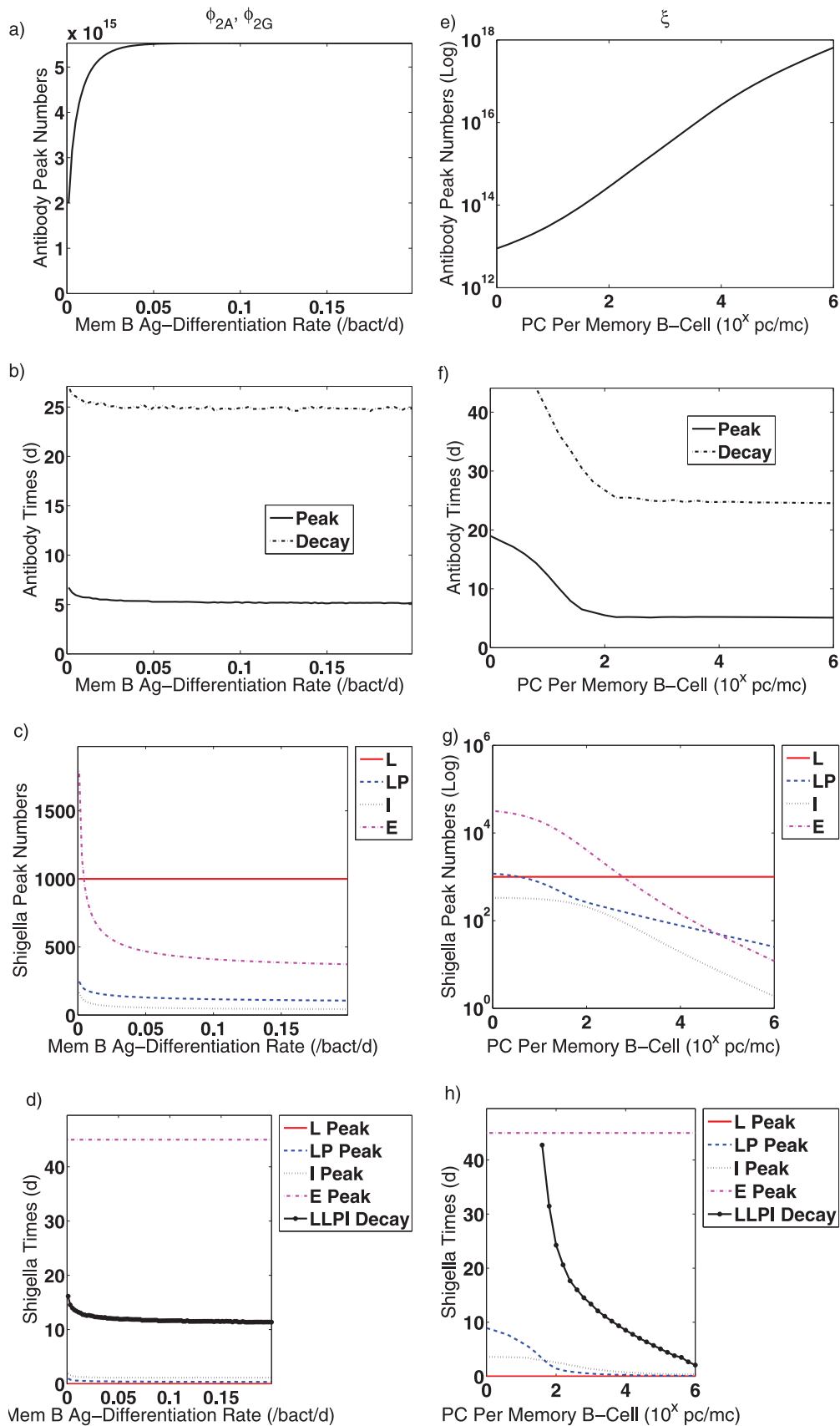


Figure 7. Effects of various parameters on post-vaccine dynamics are evaluated. Only one parameter type varies in each figure; other parameters are fixed to the values given in Table 1. (a–d) The rates that B_M differentiate into plasma cells in the presence of antigen (ϕ_{2A} and ϕ_{2G}) are varied together from 0.0001 to 0.2/bact/d. (e–f) The number of plasma cells generated by proliferating antigen-activated B_M (ζ) is varied from 1 to

10^6 pc/mc. The following results are tracked for each parameter: (a,e,f) the peak number of total antibody (lamina propria IgG plus lamina propria and luminal IgA), (b,f,j) the timing of the antibody peak, (c,g,k) the peak number of *Shigella* in the lumen (L), in the lamina propria (LP), engulfed in innate immune cells (I), and in the epithelium (E), (d,h,l) the timing of the *Shigella* peak in the aforementioned compartments as well as the time at which the total number of non-epithelial *Shigella* drops below one bacterium (LLPI Decay). Abbreviations: Ab: antibodies, d: day, bact: bacteria, pc: plasma cells, mc: memory B cells, L: lumen, LP: lamina propria, I: engulfed in innate immune cells, E: epithelium, Log: logarithmic scale, 10^x : the number on the x-axis should be used as the exponent of 10 to obtain the true value. doi:10.1371/journal.pone.0059465.g007

To explore how antigen-stimulated plasma cell creation affects bacterial and immune dynamics, we look more closely at the rates that B_M -cells differentiate into new plasma cells in response to antigen (ϕ_{2A} and ϕ_{2G}) and at the number of plasma cells created per B_M cell from this differentiation and subsequent proliferation (ξ). We vary the rates from 0.001 to 0.2 and see in Figures 7a–d that both the antibody and *Shigella* peaks are insensitive to large differentiation rates. When antigen-activated B_M cells differentiate less frequently into plasma cells, the peak magnitudes for both *Shigella* and total antibody are higher, although the peak times vary only minutely. This increased antibody production despite lower ASC creation rates demonstrates that either (1) consistent with what we have seen previously, the minor increase in the time to the antibody peak is sufficient to create more antibodies, despite a lower plasma cell creation rate or (2) antigenic stimulation of B cell generation due to higher *Shigella* levels increases sufficiently to compensate for lower B_M differentiation rates. The extinction time for non-epithelial *Shigella* drops only slightly when plasma cells are generated more quickly from B_M cells.

When we examine how the number of plasma cells made per differentiating B_M cell in the presence of antigen (ξ) affects antibody peak dynamics, we see that antibody levels rise and *Shigella* numbers decay substantially when more plasma cells are made per B_M cell (Figures 7e–h). In these figures, the value of ξ ranges from 1 to 10^6 . Here, higher antibody levels can be achieved with smaller peak times because ASC are more plentiful. Unlike with plasma cell rates, the extinction time for non-epithelial *Shigella* drops substantially when more plasma cells are generated per B_M (Figure 7h); this suggests that it is the number, not the rate, of ASC production that matters for *Shigella* clearance. Furthermore, if more than 10,000 plasma cells are created by each antigen-stimulated B_M cell differentiation and proliferation, the day-45 bacterial load in the epithelium can be contain to less than 100 bacteria (Figure 7g). This assumes a B_M carrying capacity of 1,000 cells and indicates that if the B_M homeostatic number cannot be boosted, immune protection might be achievable if the plasma-cell-generating potential of each B_M can be sufficiently increased.

To explore how the creation of new B cells from naive cells impacts infection dynamics, we first vary the creation rates of plasma cells from naive B cells (λ_{PA} , λ_{PG} , λ_{MA} , and λ_{MG}) from nearly zero (10^{-3}) to 100 plasma cells/bacteria/day. After a vaccine, both *Shigella* and antibody dynamics are completely insensitive to changes of creation rates from naive B cells since pre-existing immunity contributions dominate (not shown). Thus, we also evaluate primary infection behavior. The faster that plasma cells are created from naive B cells, the higher the antibody peak and the more swiftly it is reached during a primary infection (Figures 8a–b). The higher antibody presence has little effect on the non-epithelial *Shigella* peaks, but the bacterial peak in the epithelium is reduced (Figure 8c). Furthermore, small plasma cell creation rates can hinder *Shigella* clearance during a primary infection, but rates above 0.1 plasma cells/bacteria/day show little variation in *Shigella* extinction times (Figure 8d). Our arbitrarily chosen value of 0.1 plasma cells/bacteria/day thus results in roughly the same dynamics as far higher plasma cell creation rates.

Lastly, we investigate how the time delays used in our model influence the results. We use two time delays: (1) the time delay (τ) for new plasma cell and B_M creation from naive B cells which serves as the delay component of the differential equations and (2) a numerically enforced initial delay before naive cell activation can occur during an infection. To evaluate the impact of these delays, we consider primary infection dynamics rather than post-vaccine dynamics, as the former is where variation will be most evident. Yet, the value of the delay component built into the model (τ), which we range from 10^{-3} to 10 days, has little-to-no effect on any observed dynamics, as can be seen in Figures 8e–h. Theorizing that this might be due to the small value for the λ_s , which multiply the delayed *Shigella* numbers, we set $\lambda_{PA} = \lambda_{PG} = \lambda_{MA} = \lambda_{MG} = 100$ plasma cells/bacteria/day and reevaluated the delay effect. We again found no variation in the dynamics relative to τ . Hence, the use of delay differential equations at this stage was not essential to the observed results. However, we continue to use delay equations because it incorporates the biologically observed delay from naive B cell activation to effector or memory cell functionality without limiting our computational ability. Furthermore, it establishes a realistic modeling infrastructure that could be useful in future work.

The second delay, with which we allow the *Shigella* infection to establish for 3.5 days before naive B cell activation, does impact the results. We implement this numerically by starting an infection at either a trivial or disease-free equilibrium but running the reduced system in which we eliminate the terms for the creation of B cells from naive cells (i.e., any terms with $S_{I1}(t-\tau)$ or $S_{I2}(t-\tau)$ are set to zero) for 3.5 days. During this time, pre-existing immunity is unimpeded in its function or ability to generate new cells or antibodies. After 3.5 days, the naive cell terms are added back in and the full system runs from where the reduced system left off. When we vary this incubation time window from 10^{-3} to 10 days, Figures 8i–l result. Time delays less than one day change the dynamics little relative to one another, but longer delays increase *Shigella* peak numbers, which results in higher antibody peaks due to increased antigenic stimulation. Clearance of *Shigella* varies only slightly even when the *Shigella* peak magnitude doubles. In fact, the *Shigella* extinction time without the incubation period is identical to the 20-day extinction time with a 3.5-day incubation period. Thus, quick naive B cell activation is not vital to clearance of a *Shigella* infection.

Discussion

In this paper, we have established a mathematical framework for studying host immune interactions with *Shigella*, a dysentery-causing bacteria that kills over a million people worldwide every year. The ultimate goal of this work is to inform *Shigella* vaccine design by elucidating which immune components and bacterial targets are critical for establishing *Shigella* immunity, as “identification of the immunological correlates of protection is arguably the most crucial catalyst needed to accelerate development of effective *Shigella* vaccines” [3].

Our delay differential equation model focuses on humoral immune responses (antibodies and B cells) directed against specific

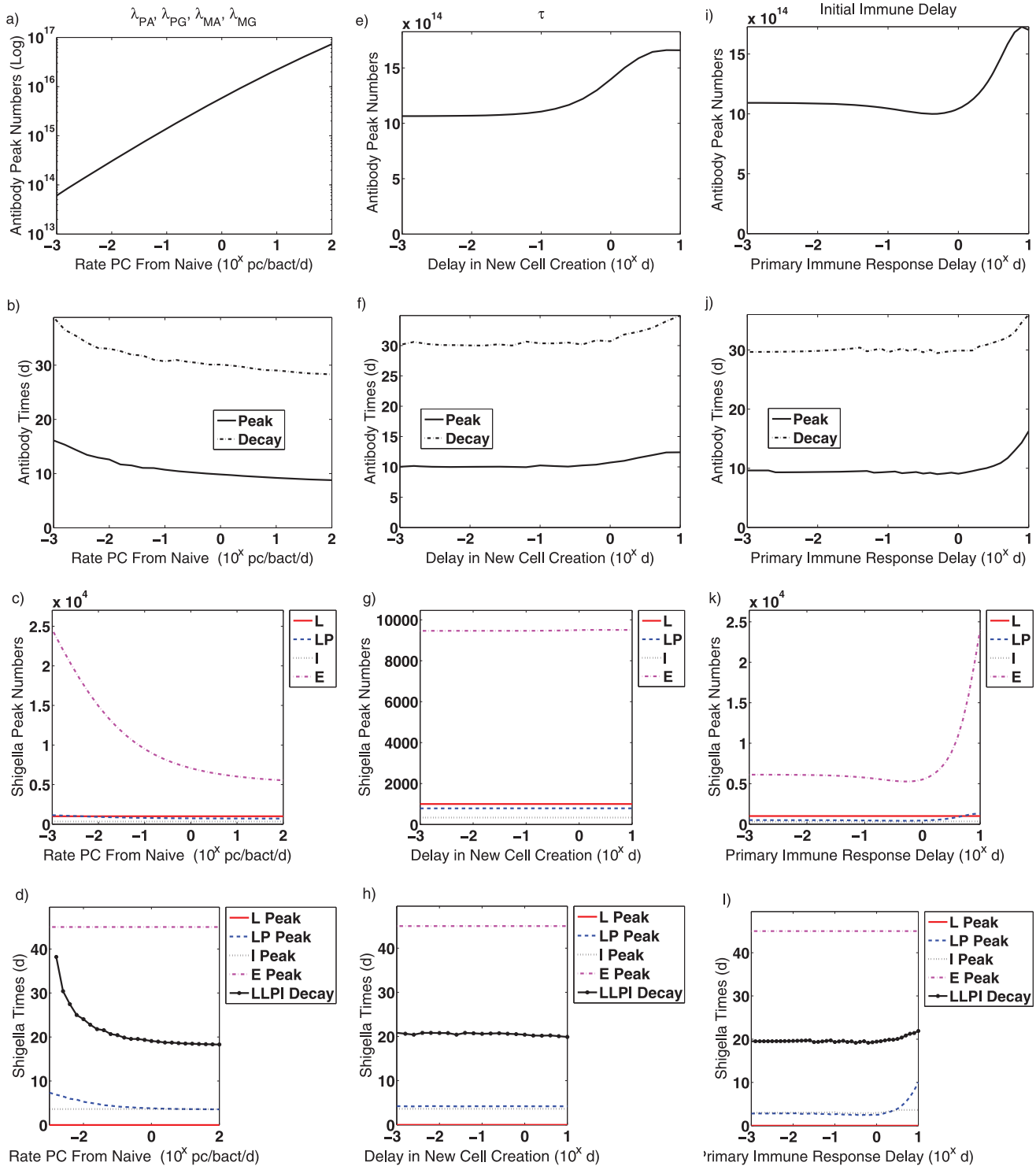


Figure 8. Effects of various parameters on primary infection dynamics are evaluated. Only one parameter type varies in each figure; other parameters are fixed to the values given in Table 1. (a–d) Creation rates of new plasma cells from naive B cells during an infection (λ_{PA} , λ_{PG} , λ_{MA} , and λ_{MG}) are varied together from 10^{-3} to 100 pc/bact/d. (e–f) The time delay for new plasma or B_M creation from naive B cells (τ) is varied from 10^{-3} to 10 d. (i–l) The initial delay until naive B cell activation in an infection is varied from 10^{-3} to 10 d. The following results are tracked for each parameter: (a,e,f) the peak number of total antibody (IgG plus IgA), (b,f,j) the timing of the antibody peak, (c,g,k) the peak number of *Shigella* in the lumen (L), in the lamina propria (LP), engulfed in innate immune cells (I), and in the epithelium (E), (d,h,l) the timing of the *Shigella* peak in the aforementioned compartments as well as the time at which the total number of non-epithelial *Shigella* drops below one bacterium (LLPI Decay). Abbreviations: Ab: antibodies, d: day, bact: bacteria, pc: plasma cells, L: lumen, LP: lamina propria, I: engulfed in innate immune cells, E: epithelium, Log: logarithmic scale, 10^x : the number on the x-axis should be used as the exponent of 10 to obtain the true value. doi:10.1371/journal.pone.0059465.g008

antigens such as LPS in *Shigella*'s outer membrane. Bacteria are targeted by anti-LPS IgG antibodies and macrophages in the lamina propria and by anti-LPS IgA antibodies in the lumen. We examine both primary infection and post-vaccine/secondary infection dynamics by initializing simulations of our model at the trivial or disease-free equilibria, respectively. Since we do not incorporate first-wave, IgM antibodies nor CMI into our model, primary infection dynamics should be viewed as a best-case approximation to actual dynamics. Equilibrium analysis and numerical simulations reveal that anti-LPS antibodies clear the lamina propria and luminal infections but are unable to prevent epithelial invasion, which causes the most severe symptoms in the host. Thus, an antibody-based vaccine targeting only surface antigens cannot elicit sufficient immunity for protection.

To explore whether a larger amount of anti-LPS antibodies than a vaccine elicits can prevent disease, we boosted IgA and/or IgG antibody numbers prior to infection via initial conditions and tracked the number of *Shigella* bacteria in the epithelium 45 days later. A primary CMI response (not modeled) in concert with a post-vaccine humoral immune response should eliminate some small amount of epithelial cell invasion, although this threshold value is unknown. However, we find that a four-orders-of-magnitude boost in IgA and IgG numbers above vaccine levels is necessary to contain the epithelial infection below a threshold of 100 bacteria, a low estimate of the minimum infectious dose in humans [19,39,40]. Furthermore, this assumes a low proliferation rate of *Shigella* inside the epithelium and thus is likely an underestimate of antibody requirements. Therefore, it will be difficult to elicit sufficient numbers of antibodies targeting only *Shigella* LPS (or other outer membrane components) to prevent shigellosis.

The caveat is that if a *Shigella* vaccine can sufficiently boost not only anti-LPS antibodies but anti-LPS B_M cells as well, the model predicts that protection might be achievable. Alternatively, if the ability of each B_M cell to generate plasma cells can be amplified, lower B_M carrying capacities might be sufficient for protection. The importance of the B_M pool in this protection indicates that anti-LPS B_M cells could be correlates of immunity for *Shigella*. However, more careful sensitivity analysis will be required to ensure that B_M cells are correlates in experimentally relevant conditions. This is a promising research avenue for future mathematical studies.

While varying the initial IgA and/or IgG levels to determine the impact of antibody boosting, we are able to determine the relative effectiveness of IgA antibodies versus IgG antibodies. Although their efficacies are closely matched, the modeling results tell us that each IgA antibody is slightly more effective than an IgG antibody. Since the model's IgA and IgG parameter values are identical, this likely results from the fact that IgA functions in the lumen and thus eliminates *Shigella* at the outset before it has the opportunity to proliferate. However, more total IgA is required than IgG to have an equal effect, because only IgA antibodies that reach the lumen contribute to this higher-per-molecule defense. A combined strategy with both IgA and IgG responses requires less total antibodies than IgA alone or IgG alone and thus is predicted to confer the best protection.

References

1. Organization WH (Mar 2009) Vaccine-Preventable Diseases and Immunization. Electronic Citation.
2. Kweon M (2008) Shigellosis: the current status of vaccine development. *Current Opinion in Infectious Diseases* 21: 313.

Since an anti-LPS antibody response is not sufficient for immunity, we extend the model non-mechanistically to explore the potential of additionally targeting *Shigella* epithelial entry proteins. We find that if IgG modulates the rate at which *Shigella* enters epithelial cells, epithelial invasion is almost entirely blocked. Thus, this vaccine strategy shows promise, yet a detailed, mechanistic model of epithelial entry that takes into account factors such as the brief availability of epithelial entry proteins is needed to better explore this avenue mathematically.

Shigella proteins involved in host cell invasion have long been considered potential vaccine targets. In fact, past vaccine trials have targeted both LPS and invasion plasmid antigens (IpaB, etc.), which play a key role in epithelial entry [43]. Thus, in future modeling, we will look more carefully at these elements to determine the mechanisms responsible for immune efficacy and to investigate other potential targets that alone or in combination can accurately predict vaccine effectiveness. Our current model thus serves as a launching point from which we can look more deeply at *Shigella* immune interactions in the future to better inform *Shigella* vaccine design.

Challenges exist in incorporating clinical data into the mathematical model. Human data are sparse in time and indirectly measured due to limited access to internal tissues, including the gastrointestinal mucosa. In addition, cut-offs for morbidity in patients are not quantitatively known, and thus it is not straight-forward to determine what bacterial loads and immune levels must be reached to achieve protection.

Our mathematical model includes many parameters that are biologically unknown (see Table 1). Our sensitivity studies are only an initial step in exploring the parameter space. While they provide insight into the role of individual parameters, much is left to be done in determining optimal clinical values and their resulting dynamics. An extensive investigation of the parameter space is beyond the scope of this work and is left to future studies and experimentation.

In summary, the mathematical model presented here explores several immune variables currently considered important in protection from *Shigella* infections. The model highlights the relative importance of the efficiency of IgA versus IgG, B_M cells versus naive B cells, and optimized efficacy with elicitation of both IgA and IgG against LPS. It is expected that highlighting the importance of these variables, including additional ones such as CMI and other *Shigella* antigens, and continued testing of the model as additional clinical data become available will accelerate the development of vaccines against *Shigella*.

Acknowledgments

We thank the volunteers that have participated in *Shigella* vaccine trials and the support of Drs. Karen Kotloff and Myron Levine that have generated clinical data that informs the development of our mathematical models.

Author Contributions

Conceived and designed the experiments: CLD RW FRT JKS MBS DL. Performed the experiments: CLD DL. Analyzed the data: CLD DL. Contributed reagents/materials/analysis tools: CLD RW FRT JKS MBS DL. Wrote the paper: CLD RW FRT JKS MBS DL.

5. Organization WH (2009). Shigellosis: Disease Burden. Electronic Citation.
6. Plotkin SA, Gilbert PB (2012) Nomenclature for immune correlates of protection after vaccination. *Clin Infect Dis* 54: 1615–7.
7. Simon J, Wahid R, Maciel M, Picking W, Kotloff K, et al. (2009) Antigen-specific B memory cell responses to lipopolysaccharide (LPS) and invasion plasmid antigen (Ipa) B elicited in volunteers vaccinated with live-attenuated *Shigella flexneri* 2a vaccine candidates. *Vaccine* 27: 565–572.
8. Simon JK, Maciel J M, Weld ED, Wahid R, Pasetti MF, et al. (2011) Antigen-specific iga b memory cell responses to shigella antigens elicited in volunteers immunized with live attenuated shigella flexneri 2a oral vaccine candidates. *Clin Immunol* 139: 185–92.
9. Ashida H, Ogawa M, Mimuro H, Kobayashi T, Sanada T, et al. (2011) *Shigella* are versatile mucosal pathogens that circumvent the host innate immune system. *Curr Opin Immunol* 23: 448–55.
10. Phalipon A, Sansonetti PJ (2007) *Shigella*'s ways of manipulating the host intestinal innate and adaptive immune system: a tool box for survival? *Immunol Cell Biol* 85: 119–29.
11. Sansonetti P, Phalipon A (1996) Shigellosis: from molecular pathogenesis of infection to protective immunity and vaccine development. *Research in Immunology* 147: 595–602.
12. Phalipon A, Sansonetti P (2003) Shigellosis: innate mechanisms of inflammatory destruction of the intestinal epithelium, adaptive immune response, and vaccine development. *Critical Reviews in Immunology* 23: 371–401.
13. Janeway C, Travers P, Walport M, Shlomchik M (2001) Immunobiology. Current Biology Publications.
14. Brandtzaeg P (2009) Mucosal immunity: induction, dissemination, and effector functions. *Scand J Immunol* 70: 505–15.
15. Baker K, Qiao SW, Kuo T, Kobayashi K, Yoshida M, et al. (2009) Immune and non-immune functions of the (not so) neonatal fc receptor, fc γ n. *Semin Immunopathol* 31: 223–36.
16. Brandtzaeg P, Johansen FE (2005) Mucosal b cells: phenotypic characteristics, transcriptional regulation, and homing properties. *Immunol Rev* 206: 32–63.
17. Brandtzaeg P (2007) Induction of secretory immunity and memory at mucosal surfaces. *Vaccine* 25: 5467–5484.
18. DuPont H, Hornick R, Snyder M, Libonati J, Formal S, et al. (1972) Immunity in shigellosis. II. Protection induced by oral live vaccine or primary infection. *J Infect Dis* 125: 12–16.
19. DuPont H, Levine M, Hornick R, Formal S (1989) Inoculum size in shigellosis and implications for expected mode of transmission. *J Infect Dis* 159: 1126–1128.
20. Raqib R, Ljungdahl A, Lindberg A, Andersson U, Andersson J (1996) Local entrapment of interferon gamma in the recovery from shigella dysenteriae type 1 infection. *Gut* 38: 328–336.
21. Raqib R, Wretling B, Andersson J, Lindberg AA (1995) Cytokine secretion in acute shigellosis is correlated to disease activity and directed more to stool than to plasma. *J Infect Dis* 171: 376–84.
22. Raqib R, Wretling B, Andersson J, Lindberg A (1995) Cytokine secretion in acute shigellosis is correlated to disease activity and directed more to stool than to plasma. *The Journal of Infectious Diseases* : 376–384.
23. Samandari T, Kotloff KL, Losonsky GA, Picking WD, Sansonetti PJ, et al. (2000) Production of ifn-gamma and il-10 to shigella invasins by mononuclear cells from volunteers orally inoculated with a shiga toxin-deleted shigella dysenteriae type 1 strain. *J Immunol* 164: 2221–32.
24. Islam D, Bardhan PK, Lindberg AA, Christensson B (1995) *Shigella* infection induces cellular activation of t and b cells and distinct species-related changes in peripheral blood lymphocyte subsets during the course of the disease. *Infect Immun* 63: 2941–9.
25. Islam D, Wretling B, Lindberg AA, Christensson B (1996) Changes in the peripheral blood t-cell receptor v beta repertoire in vivo and in vitro during shigellosis. *Infect Immun* 64: 1391–9.
26. Kotloff KL, Noriega FR, Samandari T, Szein MB, Losonsky GA, et al. (2000) *Shigella flexneri* 2a strain cvd 1207, with specific deletions in virg, sen, set, and guaba, is highly attenuated in humans. *Infect Immun* 68: 1034–9.
27. Kotloff KL, Taylor DN, Szein MB, Wasserman SS, Losonsky GA, et al. (2002) Phase i evaluation of delta virg shigella sonnei live, attenuated, oral vaccine strain wrss1 in healthy adults. *Infect Immun* 70: 2016–21.
28. Niesel DW, Hess CB, Cho YJ, Klimpel KD, Klimpel GR (1986) Natural and recombinant interferons inhibit epithelial cell invasion by shigella spp. *Infect Immun* 52: 828–33.
29. Le-Barillec K, Magalhaes J, Corcuff E, Thuizat A, Sansonetti P, et al. (2005) Roles for T and NK Cells in the innate immune response to *Shigella flexneri*. *Journal of Immunology* 175: 1735–1740.
30. Nowak M, May R (2000) Virus dynamics: mathematical principles of immunology and virology. Oxford University Press, USA.
31. Perelson A, et al. (2002) Modelling viral and immune system dynamics. *Nature Reviews Immunology* 2: 28–36.
32. Bru A, Cardona PJ (2010) Mathematical modeling of tuberculosis bacillary counts and cellular populations in the organs of infected mice. *PLoS One* 5: e12985.
33. Marino S, Linderman JJ, Kirschner DE (2011) A multifaceted approach to modeling the immune response in tuberculosis. *Wiley Interdiscip Rev Syst Biol Med* 3: 479–89.
34. Marino S, Myers A, Flynn JL, Kirschner DE (2010) Tnf and il-10 are major factors in modulation of the phagocytic cell environment in lung and lymph node in tuberculosis: a next-generation two-compartmental model. *J Theor Biol* 265: 586–98.
35. Hancioglu B, Swigon D, Clermont G (2007) A dynamical model of human immune response to influenza a virus infection. *J Theor Biol* 246: 70–86.
36. Jansen V, Korthals Altes H, Funk G, Wodarz D (2005) Contrasting b cell- and t cell-based protective vaccines. *Journal of Theoretical Biology* 234: 39–48.
37. Saul A, Fay MP (2007) Human immunity and the design of multi-component, single target vaccines. *PLoS One* 2: e850.
38. Kotloff KL, Herrington DA, Hale TL, Newland JW, Van De Verg L, et al. (1992) Safety, immunogenicity, and efficacy in monkeys and humans of invasive escherichia coli k-12 hybrid vaccine candidates expressing shigella flexneri 2a somatic antigen. *Infect Immun* 60: 2218–24.
39. Kotloff K, Losonsky G, Nataro J, Wasserman S, Hale T, et al. (1995) Evaluation of the safety, immunogenicity, and efficacy in healthy adults of four doses of live oral hybrid *Escherichia coli*-*Shigella flexneri* 2a vaccine strain EcSF2a-2. *Vaccine* 13: 495–502.
40. Kotloff K, Nataro J, Losonsky G, Wasserman S, Hale T, et al. (1995) A modified shigella volunteer challenge model in which the inoculum is administered with bicarbonate buffer: clinical experience and implications for shigella infectivity. *Vaccine* 13: 1488–1494.
41. Selge G, Magalhaes JG, Konrad C, Fritz JH, Salgado-Pabon W, et al. (2010) Th17 cells are the dominant t cell subtype primed by shigella flexneri mediating protective immunity. *J Immunol* 184: 2076–85.
42. Amanna I, Slika M (2010) Mechanisms that determine plasma cell lifespan and the duration of humoral immunity. *Immunological Reviews* 236: 125–138.
43. Riddle MS, Kaminski RW, Williams C, Porter C, Baqar S, et al. (2011) Safety and immunogenicity of an intranasal shigella flexneri 2a invaplex 50 vaccine. *Vaccine* 29: 7009–19.
44. Koterski JF, Nahvi M, Venkatesan MM, Haimovich B (2005) Virulent shigella flexneri causes damage to mitochondria and triggers necrosis in infected human monocyte-derived macrophages. *Infect Immun* 73: 504–13.
45. Cersini A, Salvia AM, Bernardini ML (1998) Intracellular multiplication and virulence of shigella flexneri auxotrophic mutants. *Infect Immun* 66: 549–57.
46. Ogawa M, Yoshimori T, Suzuki T, Sagara H, Mizushima N, et al. (2005) Escape of intracellular shigella from autophagy. *Science* 307: 727–31.
47. Levy M, Vieira P, Coutinho A, Freitas A (1987) The majority of “natural” immunoglobulin-secreting cells are short-lived and the progeny of cycling lymphocytes. *Eur J Immunol* 17: 849–854.
48. Slika M, Ahmed R (1998) Long-lived plasma cells: a mechanism for maintaining persistent anti-body production. *Curr Opin Immunol* 10: 252–258.
49. Gray D, Skarvall H (1988) B-cell memory is short-lived in the absence of antigen. *Nature* 336: 70–73.
50. Perdomo JJ, Gounon P, Sansonetti PJ (1994) Polymorphonuclear leukocyte transmigration promotes invasion of colonic epithelial monolayer by shigella flexneri. *J Clin Invest* 93: 633–43.
51. Stendahl O, Tagesson C, Magnusson KE, Edebo L (1977) Physicochemical consequences of op-sonization of *Shigella typhimurium* with hyperimmune IgG and complement. *Immunology* 32: 11–18.
52. Conrad R, Ingraham J (1974) Rate of hemolytic antibody production by single cells in vivo in rabbits. *J Immunol* 112: 17–25.
53. Helmreich E, Kern M, Eisen H (1961) The secretion of antibody by isolated lymph node cells. *J Biol Chem* 236: 464–473.
54. Helmreich E, Kern M, Eisen H (1962) Observations on the mechanism of secretion of g-globulins by isolated lymph node cells. *J Biol Chem* 237: 1925–1931.
55. Hibi T, Dosch H (1986) Limiting dilution analysis of the B cell compartment in human bone marrow. *Eur J Immunol* 16: 139–145.